0 0 0 3 4 2 0 7 3 1 3

LBL-3543
c.1

# DENSIFICATION AND ELECTRICAL PROPERTIES OF CONTROLLED STOICHIOMETRY PZT

Kenneth Edward Crabtree
(M.S. thesis)

December, 1974

Prepared for the U. S. Atomic Energy Commission
under Contract W-7405-ENG-48

RECEIVED
LAWRENCE
RADIATION LABORATORY

FEB 20 1975

LIBRARY AND
DOCUMENTS SECTION

For Reference

Not to be taken from this room

LAWRENCE BERKELEY LABORATORY
UNIVERSITY OF CALIFORNIA
BERKELEY

LBL-3543
c.1

## DISCLAIMER

This document was prepared as an account of work sponsored by the United States Government. While this document is believed to contain correct information, neither the United States Government nor any agency thereof, nor the Regents of the University of California, nor any of their employees, makes any warranty, express or implied, or assumes any legal responsibility for the accuracy, completeness, or usefulness of any information, apparatus, product, or process disclosed, or represents that its use would not infringe privately owned rights. Reference herein to any specific commercial product, process, or service by its trade name, trademark, manufacturer, or otherwise, does not necessarily constitute or imply its endorsement, recommendation, or favoring by the United States Government or any agency thereof, or the Regents of the University of California. The views and opinions of authors expressed herein do not necessarily state or reflect those of the United States Government or any agency thereof or the Regents of the University of California.

0 0 0 0 4 2 0 7 6 1 1



# DENSIFICATION AND ELECTRICAL PROPERTIES OF CONTROLLED STOICHIOMETRY PZT

Contents | Page


ABSTRACT . . . . . v

I. INTRODUCTION . . . . . 1

II. EXPERIMENTAL . . . . . 3

A. Sample Preparation . . . . . 3

B. Measurement Techniques . . . . . 5

III. RESULTS AND DISCUSSION . . . . . 7

A. Undoped $PbZr_{.5}Ti_{.5}O_3$ . . . . . 7

B. Niobium Doped $Pb_{.99}[Zr_{.49}Ti_{.49}Nb^{5+}_{.02}]O_3$ . . . . . 10

C. Tungsten Doped $Pb_{.99}[Zr_{.495}Ti_{.495}W_{.01}]O_3$ . . . . . 12

IV. CONCLUSIONS . . . . . 16

ACKNOWLEDGMENTS . . . . . 17

REFERENCES . . . . . 18

FIGURE CAPTIONS . . . . . 23

FIGURES . . . . . 24

0 0 0 0 4 2 0 7 6 1 2



# DENSIFICATION AND ELECTRICAL PROPERTIES OF CONTROLLED STOICHIOMETRY PZT

Kenneth Edward Crabtree

Inorganic Materials Research Division, Lawrence Berkeley Laboratory
and Department of Materials Science and Engineering,
College of Engineering; University of California,
Berkeley, California 94720

## ABSTRACT

The influence of a controlled PbO atmosphere during sintering on the densification and electrical properties of undoped, niobium, and tungsten doped samples of $PbZr_{.5}Ti_{.5}O_3$ was studied. Electrical properties were found to be more strongly dependent upon extrinsic than intrinsic influences within the single phase region. Substitution of $W^{6+}$ occurs at levels sufficient to neutralize any charged oxygen vacancies which may be present in the structure. Amounts in excess of this substitute by a reduction mechanism.

# I. INTRODUCTION

Outstanding ferroelectric and piezoelectric properties[1] have created considerable interest in ceramics of the pseudo-binary solid solution series $PbZrO_3$-$PbTiO_3$(PZT). Three characteristic properties of ferroelectric materials, dielectric hysteresis, piezoelectricity, and high permittivity provide many possible electrical device applications for these materials.[2] The tolerance of this system for extensive ionic substitution,[1,3-9] producing a wide variation in physical and electrical properties, affords the opportunity to manipulate these properties for specific device application. However, reproducibility of electrical properties of polycrystalline PZT ceramics has been difficult to achieve.[10,11]

Electrical properties of materials are known to be extremely sensitive to changes in microstructure and composition.[12] Effects of microstructure on electrical properties of PZT have been determined[13-17] and will not be a subject of this investigation. However, volatization of the PbO constituent[18,19] during high temperature processing determines the deviation from stoichiometry, making the final composition directly dependent upon high temperature processing parameters. This vaporization has been suppressed by hot pressing[15,20] and sintering in the presence of a PbO atmosphere of various (and varying) activities determined by a "packing powder".[1,3,8,10,18,21-23] Atkin et al.[8] found the diffusion rate of PbO in solid PZT to be comparable to the evaporation rate from the surface in air. Thus, careful use of the "packing powder" technique is necessary to assure that a constant PbO activity is maintained by the atmosphere powder in close proximity to the specimen.

Local changes in atmosphere can create unpredictable, non-reproducible changes in stoichiometry of the sample.

It became feasible to manipulate the PbO defect concentration by employing the packing powder technique when the PbO vapor pressure equilibria[24,25] and non-stoichiometry[25] in the $PbZrO_3$-$PbTiO_3$ system were determined. Vapor equilibration between a sample and a known constant PbO activity created by a multiphase packing powder would produce a sample of controlled, reproducible stoichiometry. The purpose of this work is to relate the effects of microstructure and composition on the electrical properties by employing this equilibration technique.

## II. EXPERIMENTAL

### A. Sample Preparation

The compositions chosen for this study were compounded allowing for charge compensation according to the formulas:

$$A^{2+}\ [B^{4+}]\ O_3$$

$$Pb\ [Zr_{.5}Ti_{.5}]\ O_3$$

$$Pb_{.99}\ \square_{.01}\ [Zr_{.49}Ti_{.49}Nb^{5+}_{.02}]\ O_3$$

$$Pb_{.99}\ \square_{.01}\ [Zr_{.495}Ti_{.495}W^{6+}_{.01}]\ O_3$$

(where $\square$ denotes a vacancy)

Impurity levels of the raw materials used have been shown[26] to be insufficient to effect physical and electrical properties of finished specimens. The sources of raw materials and average particle size as determined by a Fisher Sub-Sieve Sizer are listed in Table I below.

Table I. Raw materials

| Material (Supplier) | Size, μm |
|---|---|
| Reactor Grade $ZrO_2$ (Wah Chang Co.) | 9.5 |
| T.G.A. $TiO_2$ (Titanium Corp. of America) | 0.6 |
| Reagent Grade PbO (Baker Chemical) | 1.0 |
| $Nb_2O_5$ (Alfa Inorganics) | |
| $WO_3$ (Alfa Inorganics) | |

To increase reactivity of the $ZrO_2$ powder, it was milled in a neoprene lined ball mill with $ZrO_2$ balls for three days in an isopropyl alcohol medium. Average particle size was thereby reduced to 2.1 μm, and the inorganic contamination was removed by oxidation at 450°C for 10 hours.

After weighing, the raw materials were mixed for two hours using an isopropyl alochol medium in a plastic jar with $Al_2O_3$ balls to facilitate mixing and particle size reduction. After drying overnight at 80°C, the powders were isostatically pressed into a slug and air calcined in covered alumina crucibles at 1000°C for five hours. After milling under the same conditions used for mixing, the average particle size of the calcined powder was determined as listed in Table II.

Table II. Particle size of calcined powders

| Composition | Size (μm) First Calcine | Size (μm) Second Calcine |
|---|---|---|
| Undoped | 5.4 | 4.2 |
| Nb-Doped | 4.4 | 2.8 |
| W-Doped | 5.0 | 3.5 |

In order to produce more homogeneous starting material and obtain higher fired densities,[27] the material was again calcined under identical conditions. After four hours of milling under the same conditions previously used, the organic contamination was removed by oxidation and the average particle size of the double calcined powder determined (Table II). X-ray analysis showed completely reacted constituents and

sharper PZT peaks than in the initial calcine.

From these starting powders, samples were isostatically pressed into cylinders 7/16 in. diameter by 1-1/2 in. length and loaded into 99.7% alumina crucibles. Packing powders (Table III) were used to completely surround the specimens and fill the crucibles which were tightly covered to minimize PbO loss. The crucibles were then loaded side by side into a furnace which was subsequently evacuated and backfilled with pure oxygen to enhance final stage sintering.[28] At the times specified, the crucibles were cooled and specimens were cut from the slugs using a diamond saw. The remaining part of the slugs was then returned to its crucible with a fresh packing powder and sintering continued.

Table III. Packing powders

| Powder | $a_{PbO}^{1200°C}$ | $X_{PbO}$ |
|---|---|---|
| $PZ_{.5}T_{.5}$ + w/o P | .25 | 0 |
| PZ + 5 w/o Z | .08 | .020 |
| $PZ_{.5}T_{.5}$ + 5 w/o Z,T | <.035 | >.025 |

B. Measurement Techniques

Density and apparent porosity were determined by the ASTM water displacement technique.[29] Microstructures were determined using a Leitz metallograph to examine polished specimens which had been etched in a 35% solution of HCl with 5 drops of concentrated HF per 100 ml. of solution. Grain size was determined using the line intercept technique.[30]

X-ray diffraction patterns of powdered samples were taken on a Norelco diffractometer using CuK$\alpha$ radiation scanning at 1/4° per minute. Lattice parameters were determined from the center of gravity at half peak intensity.

Gold electrodes were sputtered onto specimens for electrical study. Ferroelectric data, remnant polarization ($P_R$) and coercive field ($E_c$), was determined using an "AC Looper," a modified Sawyer-Tower circuit with an oscilloscope display. During high voltage application, samples were submerged in silicone oil to prevent surface breakdown. Capacitance and dissipation factor (D) were measured on a General Radio Type 1650-A impedance bridge. Dielectric constants ($\kappa$) were calculated from capacitance data and sample dimensions using the formula:

$$\kappa = \frac{CA\varepsilon_o}{d}$$

C = measured capacitance  A = electroded area

d = sample thickness  $\varepsilon_o$ = permittivity of free space ($8.85 \times 10^{12}$ farads/meter)

## III. RESULTS AND DISCUSSION

### A. Undoped $PbZr_{.5}Ti_{.5}O_3$

The physical and electrical behavior (Table IV) of the undoped composition deviated significantly from that of intrinsic $PbZr_{.5}Ti_{.5}O_3$ because of contamination introduced during processing. Semiquantitative spectrographic analysis of powdered samples indicated that significant amounts (0.7±.4 a/o) of $Al_2O_3$ had been picked up during milling. Formation of a lead aluminate liquid phase[29] facilitates the rapid densification observed for this composition (Fig. 1).

Atkin[23] proposed oxygen vacancy compensation as the charge balancing mechanism for substitution of $Al^{3+}$ on the $[B^{4+}]$ site in PZT. He also observed that the presence of oxygen vacancies restricts grain boundary and domain mobility. A typical photomicrograph of an undoped composition is shown in Fig. 2-A. Microstructure study shows that grain growth (Fig. 3) is effectively controlled. However, discontinuous grain growth is observed (Fig. 2-B) after long times at a low PbO vapor pressure. As expected, ferroelectric activity (Fig. 4-A) is also significantly restricted.

Properties of materials fired in the low PbO activity packing powder ($PZ_{.5}T_{.5}$ + Z + T) are very sensitive to firing time. The (200) lattice spacing (Fig. 5) of these compositions was observed to decrease significantly with time. A rhombohedral phase indicating the low activity side of the single phase region[25] predominates in all compositions fired 48 hours. Deterioration of dielectric properties (Fig. 6), commensurate with increased porosity (Table IV) is explained by a series capacitance model[31] in which properties are essentially determined by the

medium of lowest permittivity.

By X-ray analysis, a small amount of a $ZrO_2$ impurity phase was detected in all specimens fired 30 hours or longer in the low PbO activity atmosphere. The development of this phase indicates that the localized PbO atmosphere surrounding the sample is not that set at the single phase boundary. The composition of the packing powder used, $PbZr_{.5}Ti_{.5}O_3$ + 5 w/o ($ZrO_2$-$TiO_2$), is actually not on the single phase boundary, but in the PZ/PT + Z primary field. Equilibrium tie lines have not been determined for this region of the ternary phase diagram. However, the phases actually present in this packing powder at high temperature are $ZrO_2$ and a titania-enriched $PZ_{.5}T_{.5}$ phase, which will determine the PbO activity of the system. Since the lead oxide activity of PZT decreases as the Zr/Ti ratio decreases,[25] the equilibrium PbO activity created by the packing powder is lower than that at the single phase boundary of $PbZr_{.5}Ti_{.5}O_3$.

The samples fired in higher PbO activity atmospheres exhibit improved properties (Table IV). The reduction of porosity (Table IV) and improved electrical properties observed with longer firing times reinforce Webster's[14] observation that porosity is the most significant factor effecting electrical properties. The increased concentration of highly polarizable $Pb^{2+}$ and $O^{2-}$ ions[32] may also exert a secondary influence in the change of dielectric constant with PbO defect concentration. Dielectric losses, indicated by the dissipation factor (Fig. 6) are lowest for these compositions.

Table IV. Measured properties of undoped $PbZr_{.5}Ti_{.5}O_3$

| Packing Powder | Time (hrs) | Apparent Density | Apparent Porosity (%) | Grain Size (μm) | κ | D(%) | $P_R$ $\left(\frac{\mu coul.}{cm^2}\right)$ | $E_C$ $\left(\frac{kV}{cm}\right)$ | (200) Lattice Spacing (Å) | (002) Lattice Spacing (Å) |
|---|---|---|---|---|---|---|---|---|---|---|
| PZT + P | 15 | 7.70 | 0.6 | 15 | 723 | 0.5 | 1.9 | 5 | 2.012 | 2.073 |
| | 30 | 7.85 | 0.2 | 17 | 802 | 0.3 | 3.1 | 5 | 2.015 | 2.068 |
| | 48 | 7.90 | 0.2 | 19 | 1017 | 0.5 | 8 | 4 | 2.019 | 2.075 |
| PZ + Z | 15 | 7.99 | 0.4 | 8 | 826 | 0.4 | 9.5 | 4.3 | 2.014 | 2.069 |
| | 30 | 8.03 | 0.2 | 14 | 983 | 0.8 | 5.6 | 3 | 2.016 | 2.069 |
| | 48 | 7.98 | 0.5 | 19 | 1040 | 0.8 | 4.7 | 2.5 | 2.013 | 2.070 |
| PZT + Z + T | 15 | 7.85 | 0.5 | 8.5 | 701 | 0.7 | 1 | 1.8 | 2.014 | 2.069 |
| | 30 | 7.73 | 1.4 | 9 | 441 | 1.0 | 3.8 | 5.5 | 2.013 | 2.071 |
| | 48 | 7.62 | 4.9 | 10 | 181 | 2.2 | 1.6 | 6.0 | Rhomb 2.008 | 2.070 |



0 0 0 0 4 2 0 7 6 1 7

B. Niobium Doped $Pb_{.99}[Zr_{.49}Ti_{.49}Nb^{5+}_{.02}]O_3$

Substitution of $Nb^{5+}$ onto the $[B^{4+}]$ site of PZT is compensated by charged lead vacancies which increase domain boundary mobility.[31] Presence of the $Al^{3+}$ impurity in comparable concentrations will create a compensating effect.[23] However, spectrographic analysis indicates that the dopant concentration of $Nb^{5+}$ (1.0±.5 a/o) is sufficient to exceed the level of compensation for $Al^{3+}$. In agreement with previous studies,[8,23,25,26,31] $Nb^{5+}$ is observed to be an effective grain growth inhibitor (Fig. 3).

Properties (Table V) of samples fired 15 hours in atmospheres of different PbO activity remained remarkably insensitive to this variable. X-ray studies of samples fired in the low PbO activity packing powder (expected to form a two-phase material at equilibrium) indicates that the process of equilibration is occurring at a much slower rate than densification. The qualitative variation in electrical properties of discs from different locations on a fired slug indicates that a specimen of this particular sample geometry essentially creates its own equilibrium atmosphere at short firing times.

At extended firing times in a low PbO activity atmosphere, deterioration of electrical properties (Fig. 6) accompanies the formation of a two-phase material with increased porosity. The higher PbO activity atmospheres produced consistently excellent properties (Table V). While other properties were comparable, the high activity side of the single phase region (PZT + P) exhibits higher dielectric constants, lower coercive fields and lower remnant polarization than samples fired in a

Table V. Measured properties of niobium doped $PZ_{.5}T_{.5}$

| Packing Powder | Time (hrs) | Apparent Density | Apparent Porosity (%) | Grain Size (μm) | κ | D(%) | $P_R$ $\left(\frac{\mu coul.}{cm^2}\right)$ | $E_C$ $\left(\frac{kV}{cm}\right)$ | (200) Lattice Spacing (Å) | (002) Lattice Spacing (Å) |
|---|---|---|---|---|---|---|---|---|---|---|
| PZT + P | 15 | 7.97 | 0.3 | 4 | 859 | 1.7 | 22 | 7.2 | 2.013 | 2.066 |
| | 30 | 8.04 | 0.3 | 7.7 | 983 | 1.7 | 20 | 6.9 | 2.013 | 2.068 |
| | 48 | 8.05 | 0.2 | 1.1 | 1062 | 1.7 | 23 | 7.0 | 2.013 | 2.068 |
| PZ + Z | 15 | 7.96 | 0.4 | 6.5 | 849 | 1.8 | 27 | 9.3 | 2.013 | 2.070 |
| | 30 | 8.00 | 0.3 | 8.3 | 791 | 1.4 | 25 | 10.4 | 2.015 | 2.070 |
| | 48 | 8.01 | 1.0 | 8.5 | 904 | 1.7 | 25 | 10.5 | 2.013 | 2.069 |
| PZT + Z + T | 15 | 7.87 | 5.5 | 9.8 | 847 | 1.6 | 27 | 9.1 | 2.013 | 2.067 |
| | 30 | 7.79 | 9.6 | 12.5 | 384 | 1.8 | 13 | 9.4 | 2.010 | 2.067 |
| | 48 | 7.69 | 12.1 | 13.5 | 373 | 4 | 7 | 10.3 | Rhomb 2.006 | 2.065 |



0 0 0 0 4 2 0 7 6 1 8

PZ + Z controlled atmosphere.

C. Tungsten Doped $Pb_{.99}[Zr_{.495}Ti_{.495}W_{.01}]O_3$

Substitution of $W^{6+}$ (.62 Å) is expected to occur on the $[B^{4+}]$ site in PZT in conjunction with a charge compensating lead vacancy. This has been substantiated by the observation of decreased mechanical quality factor,[33,34] caused by the presence of lead vacancies[6] formed during $W^{6+}$ substitution. In agreement with the model proposed by Atkin,[23] Takahashi observed[33,35] tungsten to be an effective grain growth inhibitor.

The results of this study are in opposition to this observation. Tungsten was found to be an ineffective grain growth inhibitor (Fig. 3). Thus, a mechanism of substitution of $W^{6+}$ into the PZT lattice must be proposed to account for the observations of this study.

The multivalence (+2, +3, +4, +5, +6) of the tungsten atom presents a likely explanation for this observation. The natural tendency of atoms to reduce at high temperatures suggests that such a compensating mechanism for $W^{6+}$ substitution may occur. The principal valence states for tungsten are +4 and +6. The equilibrium vapor of oxygen, calculated from JANAF data for the reaction

$$WO_{2.72} \xrightarrow{1200°C} WO_2 + .36\ O_2$$

is 26.3 atmospheres.[36] The rules of crystal chemistry would also favor substitution of $W^{4+}$ (.70 Å) rather than $W^{6+}$ (.62 Å), which is actually at the limits of compatibility with the perovskite structure. Apparently the energy required to reduce tungsten is less than that necessary to create charged vacancies in the PZT structure. Thus, sufficient amounts

of $W^{6+}$ substitute in the structure to compensate for the presence of $Al^{3+}$; the rest is reduced to $W^{4+}$ which would not be expected to influence grain boundary mobility.

Similarities between properties of pure $PbZr_{.5}Ti_{.5}O_3$ and the tungsten doped ceramics of this study support the theory of valence reduction. Close agreement between lattice constants (Fig. 5) of tungsten doped $PbZr_{.5}Ti_{.5}O_3$ and those of intrinsic material[37] implies a compatibility between the lattice and a substituting tungsten ion which would not be expected for $W^{6+}$ at .62 Å. Ferroelectric properties $P_R$ and $E_c$ of undoped $PbZr_{.5}Ti_{.5}O_3$[38] are strikingly similar to those of the tungsten doped samples of this study (Table VI). The presence of lead vacancies produced by substitution of $W^{6+}$ would facilitate switching, producing a square looped material.[23] However, the intrinsic shape of the ferroelectric loops (Fig. 4-C) observed for tungsten doped materials in this study further substantiates a self-compensating substitution mechanism.

While evidence is strong for valence compensation, the diffusivity of the solute in relation to the velocity of grain boundary motion will determine its degree of influence on densification. If the velocity of the grain boundary is low relative to the diffusivity of the solute ion, the drag effect would be negligible.[39] The diffusivity of a $W^{6+}$ ion with its associated lead vacancy could easily be greater than that of a complex of two $Nb^{5+}$ ions and their associated lead vacancy. Increased mobility may thus render tungsten an ineffective grain growth inhibitor; however, this mechanism does not explain electrical behavior.

Table VI. W doped

| Packing Powder | Time (hrs) | Apparent Density | Apparent Porosity (%) | Grain Size (μm) | K | D(%) | $P_R$ $\left(\frac{\mu coul.}{cm^2}\right)$ | $E_C$ $\left(\frac{kV}{cm}\right)$ | (200) Lattice Spacing (Å) | (002) Lattice Spacing (Å) |
|---|---|---|---|---|---|---|---|---|---|---|
| PZT + P | 15 | 7.94 | 0.4 | 26 | 465 | 2.2 | 8.5 | 1.0 | 2.015 | 2.074 |
| | 30 | 7.89 | 0.2 | 32 | 520 | 2.1 | 8.5 | 8.3 | 2.016 | 2.073 |
| | 48 | 7.88 | 0.3 | 38 | 926 | 1.5 | 14.0 | 5.1 | 2.015 | 2.072 |
| PZ + Z | 15 | 7.97 | 0.5 | 24 | 440 | 2.0 | 9.0 | 9.3 | 2.016 | 2.074 |
| | 30 | 7.97 | 0.6 | 32 | 439 | 1.5 | 8.5 | 9.3 | 2.019 | 2.074 |
| | 48 | 7.88 | 0.4 | 38 | 734 | 1.3 | 9 | 9.1 | 2.015 | 2.072 |
| PZT + Z + T | 15 | 7.85 | 10.9 | 25 | 305 | 1.5 | 4 | 9.5 | 2.011 | 2.070 |
| | 30 | 7.74 | 20.5 | 40 | 169 | 3.6 | 4 | 9.5 | 2.009 | 2.070 |
| | 48 | 7.65 | 31.7 | - | 23 | 5.4 | 3.5 | 9.7 | Rhomb 2.008 | 2.068 |

Densities of tungsten doped specimens were observed to decrease with extended firing in all atmospheres. These results are greatly accentuated in the low activity powder ($PZ_{.5}T_{.5}$ + Z + T). Poor mechanical strength of specimens fired 48 hours in this atmosphere made microstructure determinations impossible. Lattice spacings (Fig. 5) and dielectric properties (Fig. 6) also deteriorated rapidly.

## IV. CONCLUSIONS

(1) Substitution of $W^{6+}$ occurs at levels sufficient to neutralize any charged oxygen vacancies which may be present in the structure. Amounts in excess of this substitute as $W^{4+}$ by a reduction mechanism.

(2) Electrical properties were found to be more strongly dependent upon extrinsic than intrinsic influences within the single phase region.

(3) For the particular sample geometry studied, the effect of a low PbO atmosphere ($a_{PbO}^{1200°C}$ <.034) on electrical properties after short sintering times is negligible.

0 0 0 0 4 2 0 7 6 2 1



ACKNOWLEDGEMENTS

I wish to express my sincere thanks to my advisor, Professor R. M. Fulrath, without whose tolerance and guidance this work could never have been done. The encouragement and helpful assistance of my fellow graduate students was also instrumental in this work. Technical assistance from Kelly Radmilovic, Walt Toutolmin, Jack Wodei, Doug Kreitz and Lee Johnson is greatfully acknowledged. Discussions with John Sherohman were immeasurably helpful.

This work was done under the auspices of the U. S. Atomic Energy Commission.

REFERENCES

1. Jaffe, Roth, and Marzullo, "Properties of Piezoelectric Ceramics in the Solid Solution Series Lead Titanate-Lead Zirconate-Lead Oxide: Tin Oxide and Lead Titanate-Lead Hafnate," J. Appl. Phys. 25 [6] 809-10 (1954).

2. Kell, R. C., "Modern Applications of Ferroelectricity," J. Appl. Phys. 14 249-55 (1963).

3. Kulcsar, F., "Electromechanical Properties of Lead Titanate-Zirconate Ceramics with Lead Partially Replaced by Calcium or Strontium," J. Am. Ceram. Soc 42 [1] 49-51 (1959).

4. Kulcsar, F., "Electromechanical Properties of Lead Titanate-Zirconate Ceramics Modified with Certain Three-or-Five-Valent Additions," J. Am. Ceram. Soc. 42 [7] 343-349 (1959).

5. Kulcsar, F., "Electromechanical Properties of Lead Titanate-Zirconate Ceramics Modified with Tungsten and Thorium," J. Am. Ceram. Soc. 48 [1] 54 (1965).

6. Gerson, R., "Variation in Ferroelectric Characteristics of Lead Zirconate Titanate Ceramics Due to Minor Chemical Modifications," J. Appl. Phys. 31 [1] 188-94 (1960).

7. Jaffe, H., "Properties of Ferroelectric Ceramics in the Lead Titanate-Zirconate System," Inst. of Elect. Engrs. Paper No. 3625, June 1961.

8. Atkin, Holman, and Fulrath, "Substitution of BiO and Nb Ions in Lead Zirconate-Titanate," J. Am. Ceram. Soc. 54 [2] (1971).

9. Berlincourt, Cmolik, Jaffe, "Piezoelectric Properties of Polycrystalline Lead Titanate-Zirconate Compositions," Proc. IRE, 48, Feb. 1960, pp. 220-229.

10. Weston, T. B., "Studies in the Preparation and Properties of Lead Zirconate-Lead Titanate Ceramics," Canada Dept. Mines & Tech. Surveys, Mineral Processing Div. Internal Rept. MPI 63-7, Jan. 1963.

11. Weiler, J. E., "Lead Zirconate Titanate Process Development," Titanium Alloy Mfg. Div., Nat'l Lead Co. Pilot Scale Investigation RD-342, May 1968.

12. Kingery, W. D., Introduction to Ceramics, p. 647, Wiley & Sons.

13. Jonker and Stuijts, "Controlling the Properties of Electroceramic Materials Through Their Microstructure," Philips Tech. Rev. 32, No. 3/4, 79-95 (1971).

14. Webster, A. H., "Effects of Some Fabrication Conditions on the Properties of Lead Zirconate-Titanate Ceramics," Canada Dept. of Mines and Tech. Surveys, Mines Branch Investigation Report IR 63-59, July 1963.

15. Haertling, G. H., "Hot Pressed Lead Zirconate-Lead Titanate Ceramics Containing Bismuth," J. Am. Ceram. Soc. 43 [12] 875-9 (1964).

16. Gerson and Marshall, "Dielectric Breakdown of Porous Ceramics," J. Appl. Phys. 30 11 (1959).

17. Okazaki, Nagata, "Effects of Density and Grain Size of Piezoelectric Ceramics upon Electrical Properties," Trans. Inst. Elect. & Comm. Engrs. of Japan 53-C, 11, 815-22 (1970).

18. Levett, P. D., "Factors Affecting Lead Zirconate-Lead Titanate Ceramics," Am. Ceram. Soc. Bull. 42 [6] 348-52 (1963).

19. Webster, Weston, and Bricht, "Effect of PbO Deficiency on the Piezoelectric Properties of Lead Zirconate-Titanate Ceramics," J. Am. Ceram. Soc. 50 [9] 490-1 (1967).

20. Semans, B., "Densification and Electrical Properties of Lead Zirconate-Titanate," M.S. Thesis, Univ. of Calif. Berkeley (1968) (UCRL-18126).

21. Snow, G. S., "Fabrication of Electro-optic PLZT by Atmosphere Sintering," Sandia Laboratories Dev. Report SC-DR-72-0600 Sept. 1972.

22. Dungan, Barnett, and Stark, "Phase Relations and Electrical Parameters in the Ferroelectric-Antiferroelectric Region on the System $PbZrO_3$-$PbTiO_3$-$PbNb_2O_6$," J. Am. Ceram. Soc. 45 [8] 382-8 (1962).

23. Atkin and Fulrath, "Point Defects and Sintering of Lead Zirconate-Titanate," J. Am. Ceram. Soc. 54 [5] 265-70 (1971).

24. Hardtl and Rau, "PbO Vapor Pressure in the $Pb(Ti_{1-x}Zr_x)O_3$ System," Solid State Communications, 7 41-5 (1969).

25. Holman, R. L., "Intrinsic and Extrinsic Non-Stoichiometry in the Lead Zirconate-Titanate System," Ph.D. Thesis, Univ. of Calif. Berkeley (1972) (LBL-880).

26. Lee, D. C., "Sintering Sc and Nb Modified PZT," M.S. Thesis, Univ. of Calif., Berkeley (1970) UCRL-19188.

27. Seider and Koenig, "Solid Solution Reactions of Certain Lead Compositions and Compounds," Rutgers University School of Ceramics Project No. LC-21 Report #3 (1965).

0 0 0 0 4 2 0 7 6 2 3



28. Pryor, G. A., "Impurity Effects in Sintering PZT," M.S. Thesis, Univ. of Calif., Berkeley, UCRL-18191 (1968).

29. ASTM Designation C20-46 (1961) 1964 Book of ASTM Stds Part 13 Publ. by ASTM.

30. Hilliard, John E., "Estimating Grain Size by the Intercept Method," Metal Progr., 85 [5] 99-102 (1964).

31. Atkin, R. B., "Sintering and Ferroelectric Properties of Lead Zirconate Titanate Ceramics," D. Eng. Thesis, Univ. of Calif. Berkeley, 1970, UCRL-20309.

32. Roberts, Shepard, "Polarizabilities of Ions in Perovskite-Type Crystals," Phys. Rev., 81 [5] 865-68 (1951).

33. Takahaski, S. and Takahashi, M., "Effects of Impurities on Mechanical Quality Factor of PZT Ceramics," Japan J. Appl. Phys., 11 [1] (1972) p. 31.

34. Banno and Tsunooka, "Piezoelectric Properties and Temperature Dependences of Resonant Frequency of $WO_3$-$MnO_2$-Modified Ceramics of $Pb(Zr\text{-}Ti)O_3$ Ceramics," Japan J. Appl. Phys. 6 [8] 954-62 (1967).

35. Takahashi, M., "Space Charge Effect in PZT Ceramics Caused by the Addition of Impurities," Japan J. Appl. Phys. 9 [10] (1970) p. 1236.

36. Prof. A. W. Searcy, private communication.

37. Moon, Ronald L., "High Temperature Phase Equilibria in the Lead Titanate-Lead Zirconate System," Ph.D. Thesis, Univ. of Calif. Berkeley, 1967, UCRL-17545.

38. Sherohman, John, "Liquid Phase Densification of PZT," Ph.D. Thesis, Univ. of Calif., Berkeley, 1974, LBL-2767.

39. Cahn, John W., "The Impurity-Drag Effect in Grain Boundary Motion," Acta Met. 10 789-98 (1962).

FIGURE CAPTIONS

Fig. 1. Densification vs Time $^{1/2}$ at 1200°C.

Fig. 2. Typical microstructures of undoped $PbZr_{.5}Ti_{.5}O_3$.

(A) Undoped, fired 15 hrs in PZT + Z + T atm.

(B) Undoped, fired 48 hrs in PZT + Z + T atm.

Fig. 3. Grain size vs log time.

Fig. 4. Typical ferroelectric loops.

Fig. 5. Lattice spacings vs PbO defect concentration.

(A) Undoped.

(B) Nb doped.

(C) W doped.

Fig. 6. Dielectric properties vs PbO defect concentration.

(A) Undoped.

(B) Nb doped.

(C) W doped.

Fig. 7. Typical microstructures of doped $PbZr_{.5}Ti_{.5}O_3$.

(A) $Pb(Zr_{.49}Ti_{.49}Nb_{.02})O_3$ fired 48 hrs in PZ + Z atm.

(B) $Pb(Zr_{.495}Ti_{.495}W_{.01})O_3$ fired 30 hrs in PZT + P atm.

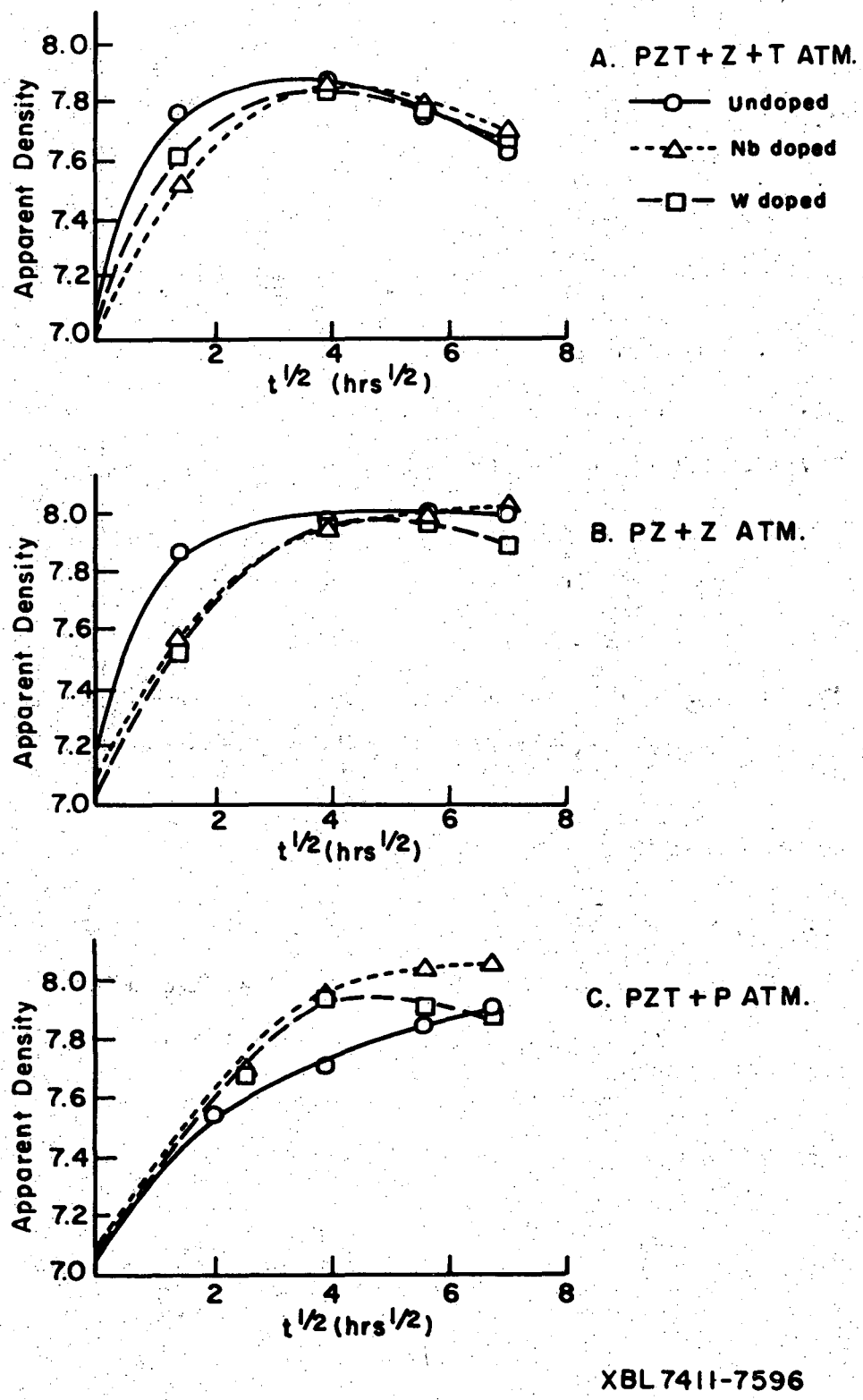
A. PZT + Z + T ATM.
Undoped
Nb doped
W doped
Apparent Density
8.0
7.8
7.6
7.4
7.2
7.0
2
4
6
8
t 1/2 (hrs 1/2)
B. PZ + Z ATM.
Apparent Density
t 1/2 (hrs 1/2)
C. PZT + P ATM.
Apparent Density
t 1/2 (hrs 1/2)
XBL 7411-7596

Fig. 1

0 0 0 0 4 2 0 7 6 2 5

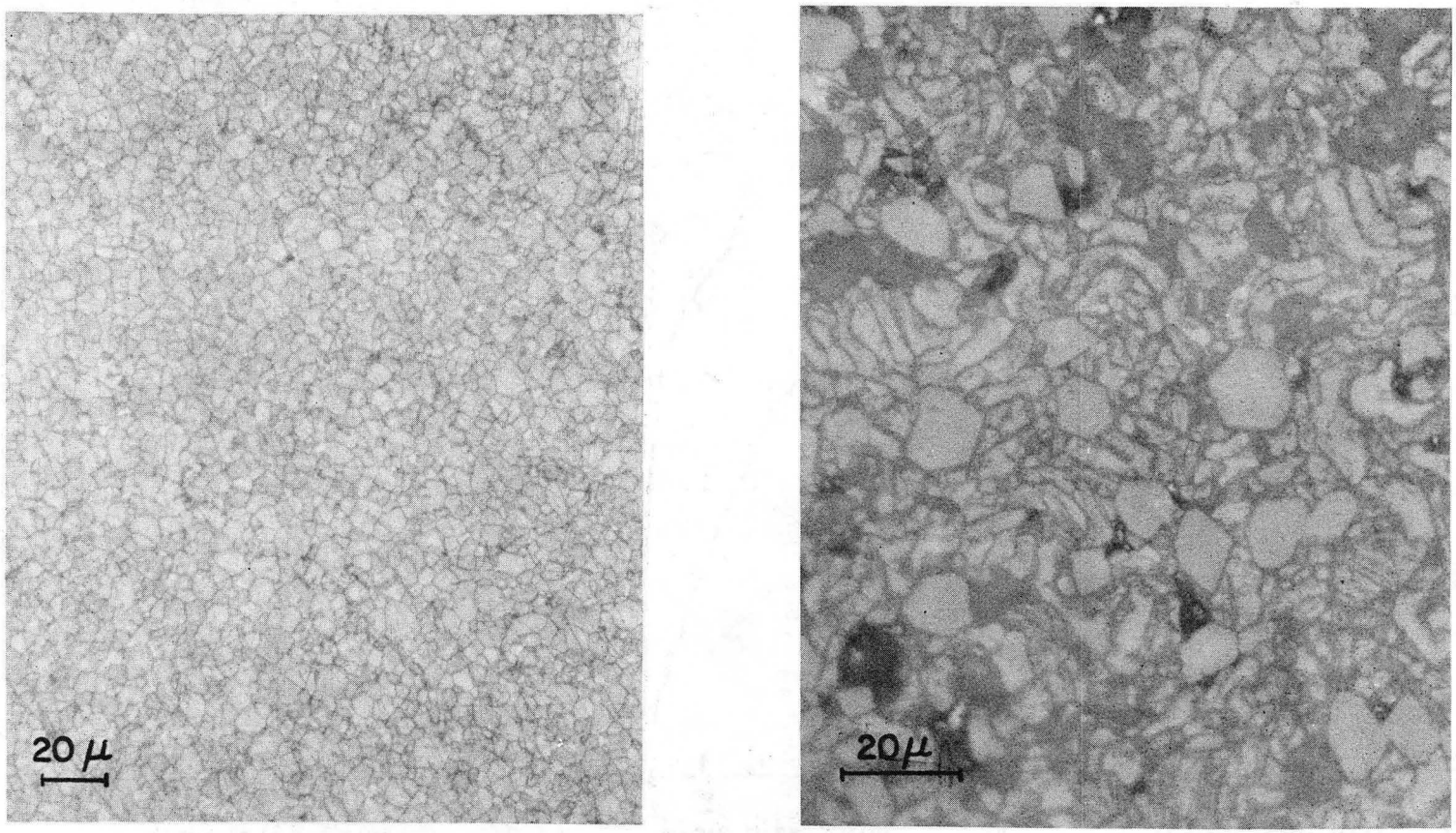


XBB 7411-8283

Fig. 2

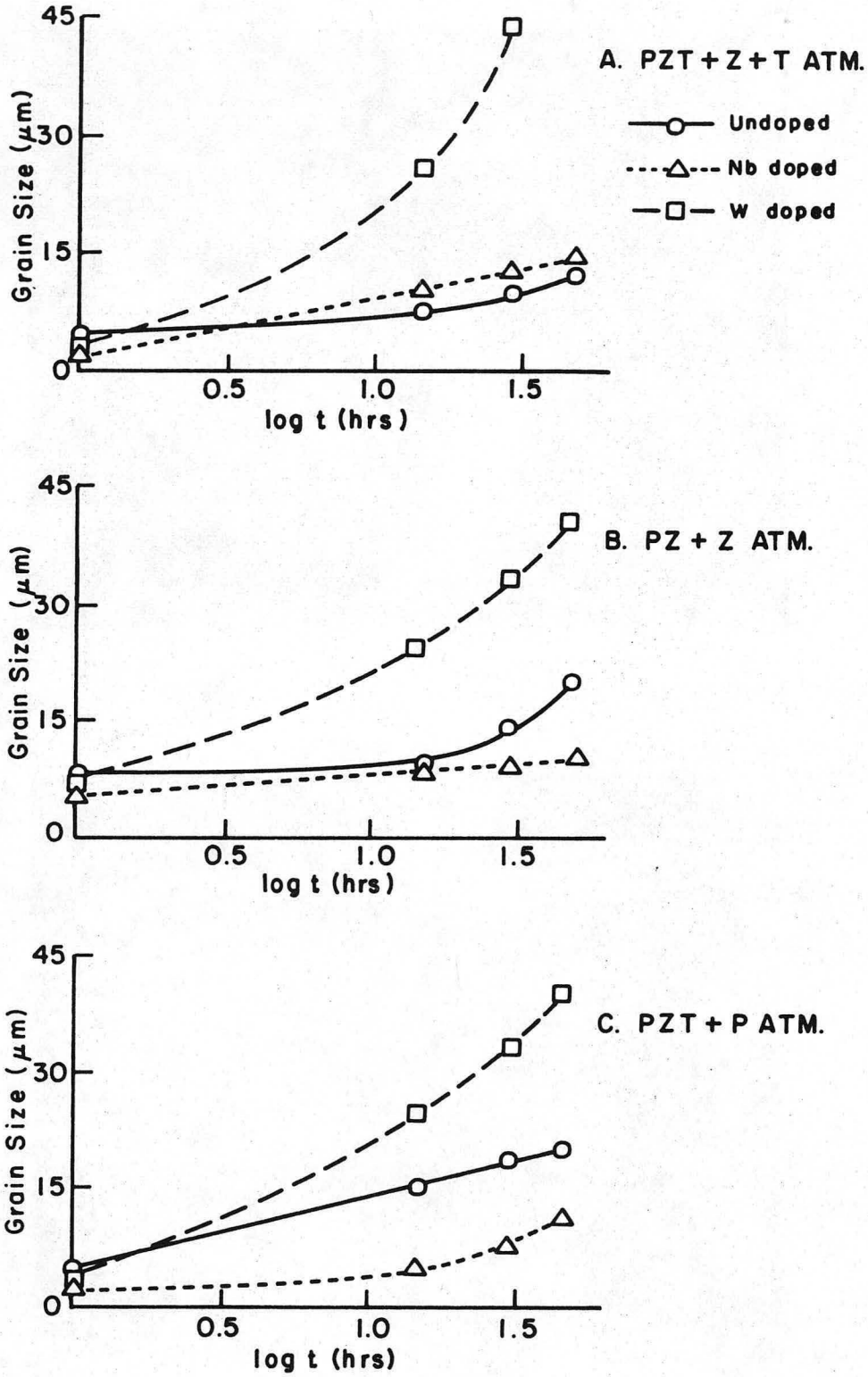


XBL 7411-7597

Fig. 3

0 0 0 0 4 2 0 7 6 2 6



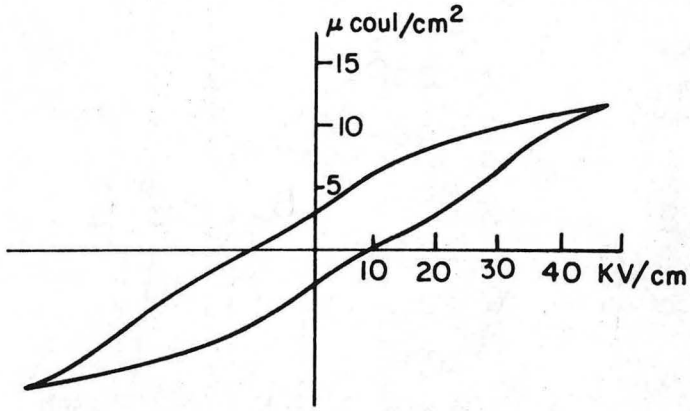


A. UNDOPED

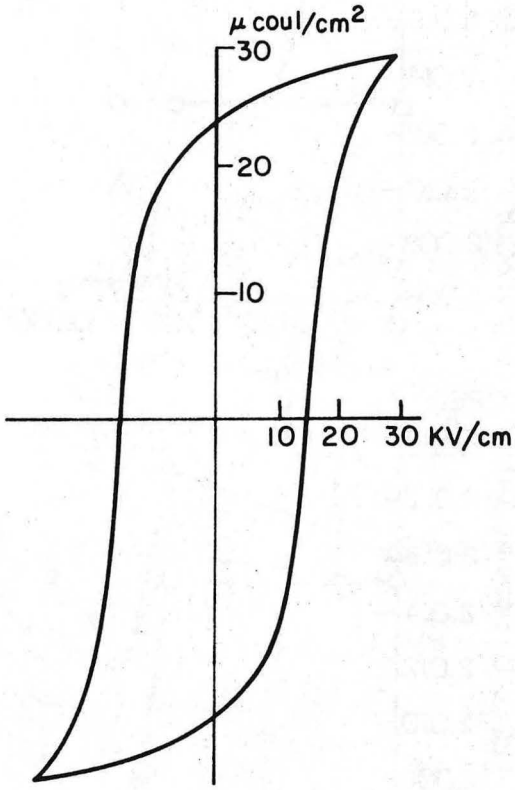


B. Nb DOPED

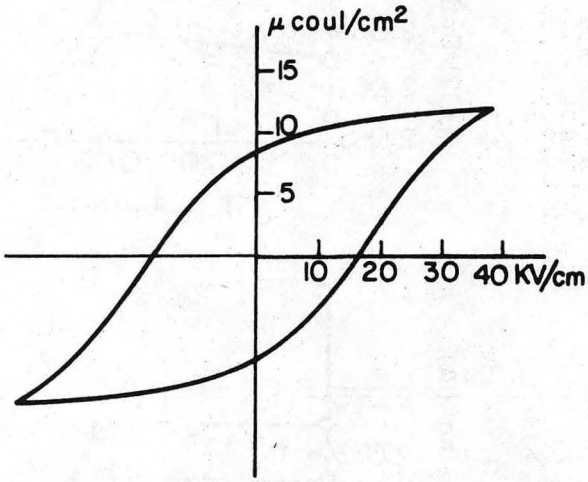


C. W DOPED

XBL 7411-7600

Fig. 4

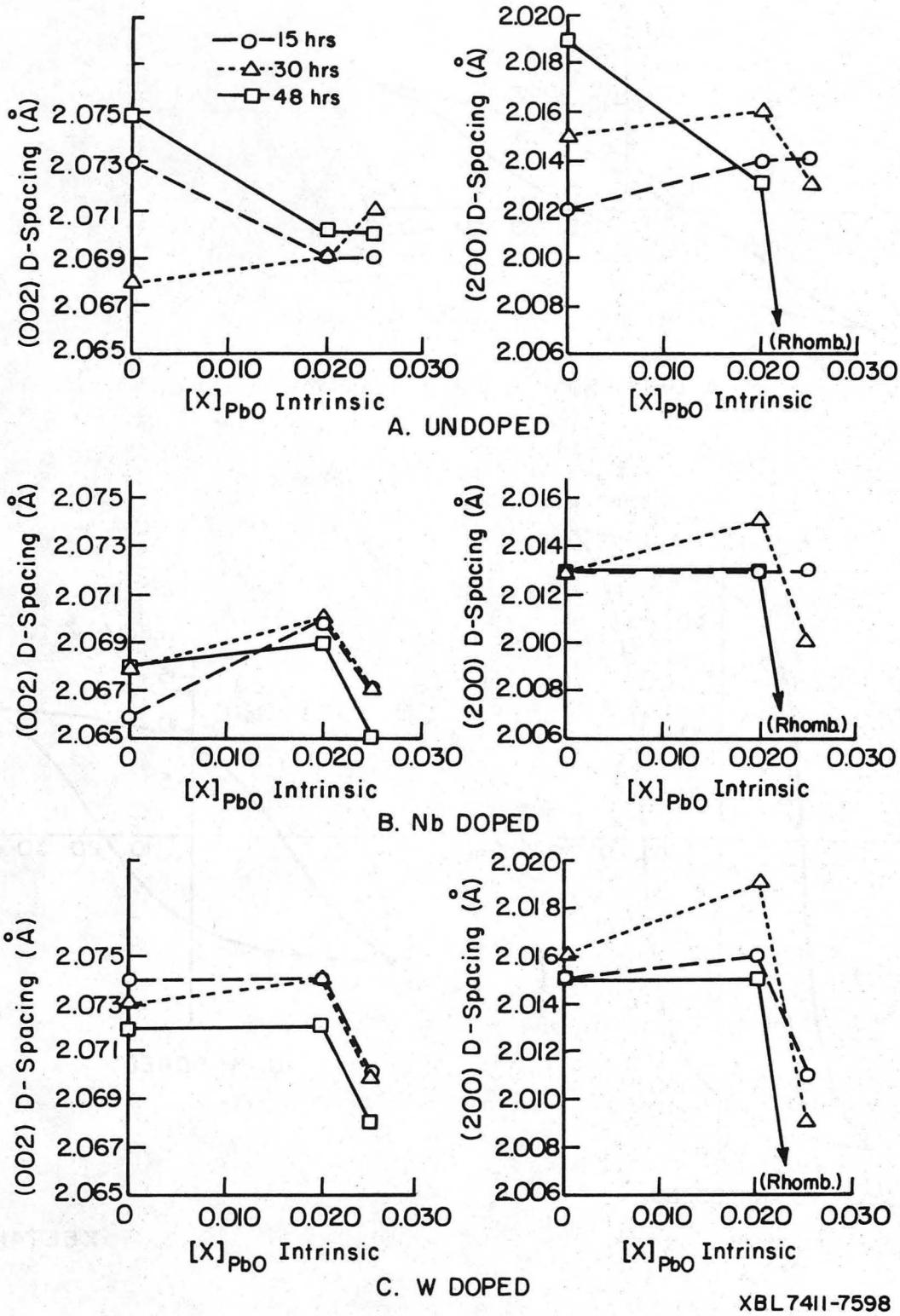
—o—15 hrs
--Δ--30 hrs
—□—48 hrs
(002) D-Spacing (Å)
2.075
2.073
2.071
2.069
2.067
2.065
0
0.010
0.020
0.030
[X]PbO Intrinsic
(200) D-Spacing (Å)
2.020
2.018
2.016
2.014
2.012
2.010
2.008
2.006
(Rhomb.)
A. UNDOPED
B. Nb DOPED
C. W DOPED
XBL7411-7598

Fig. 5

0 0 0 0 4 2 0 7 6 2 7



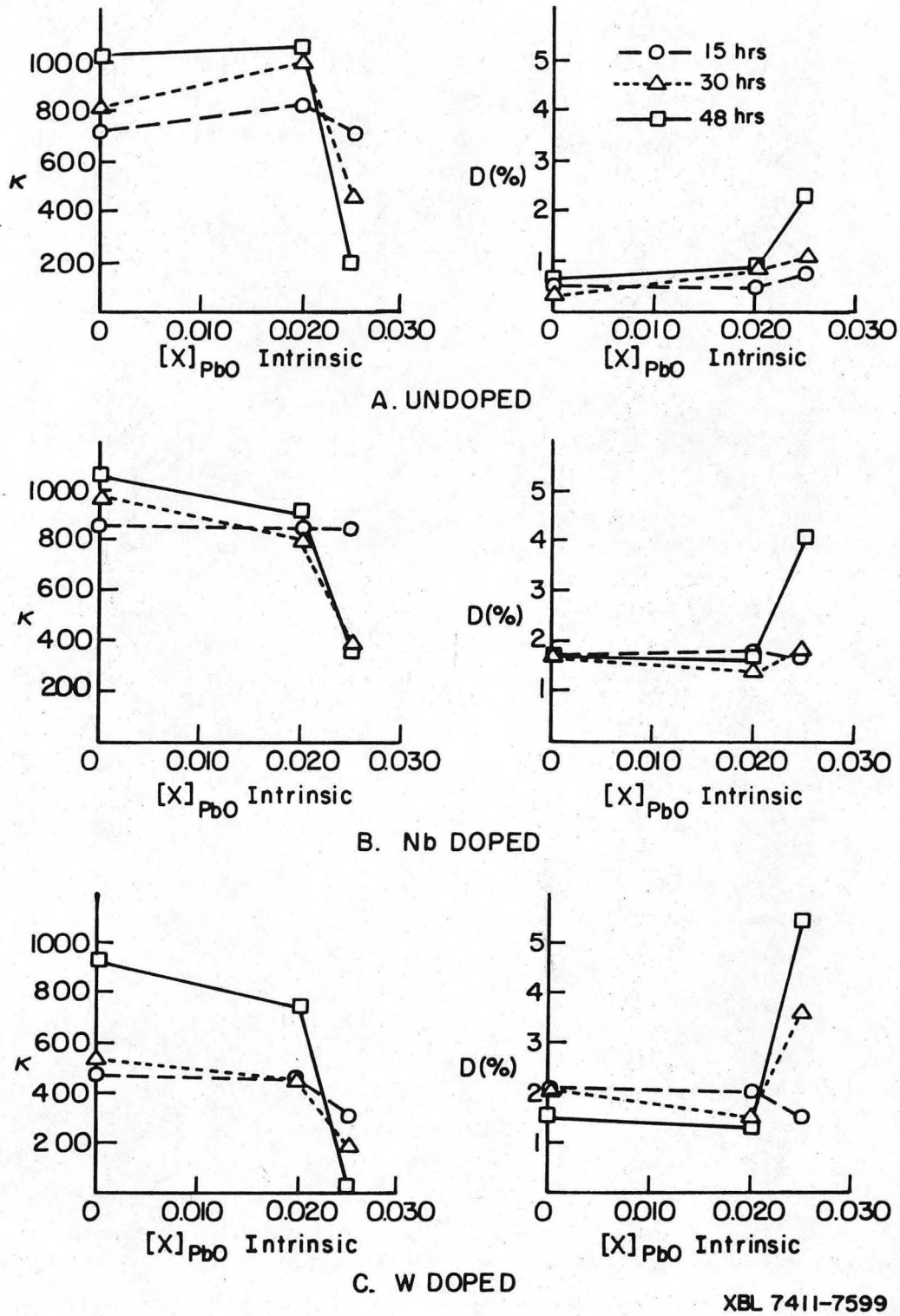


Fig. 6

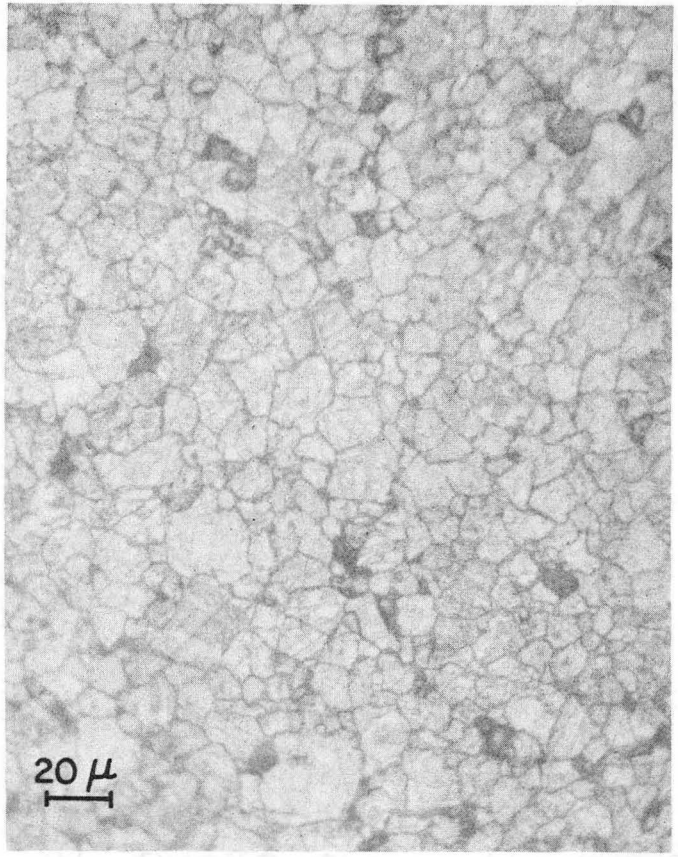


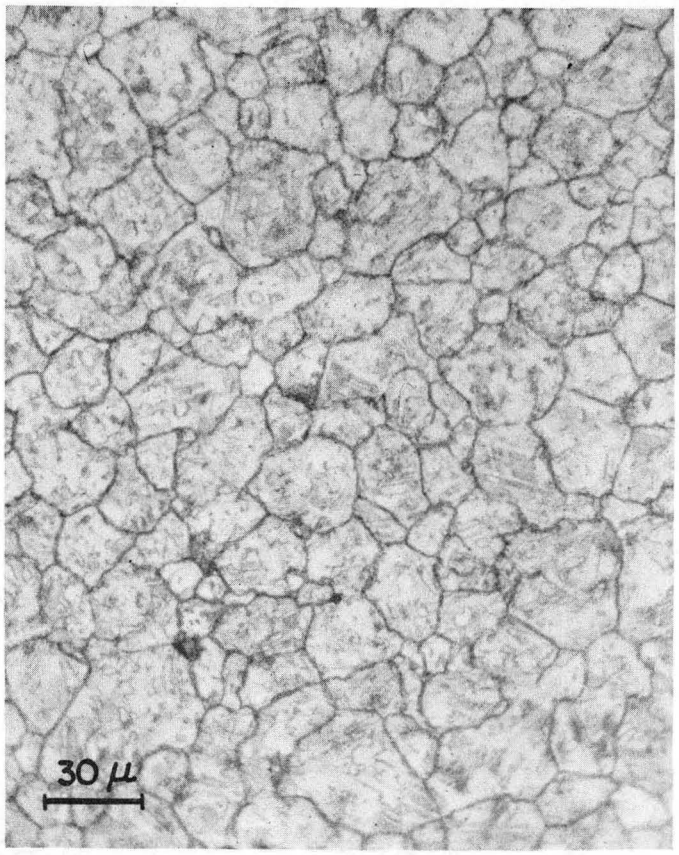


XBB 7411-8282

Fig. 7

0 0 0 0 4 2 0 7 6 2 8

LEGAL NOTICE

*This report was prepared as an account of work sponsored by the United States Government. Neither the United States nor the United States Atomic Energy Commission, nor any of their employees, nor any of their contractors, subcontractors, or their employees, makes any warranty, express or implied, or assumes any legal liability or responsibility for the accuracy, completeness or usefulness of any information, apparatus, product or process disclosed, or represents that its use would not infringe privately owned rights.*

*TECHNICAL INFORMATION DIVISION*
*LAWRENCE BERKELEY LABORATORY*
*UNIVERSITY OF CALIFORNIA*
*BERKELEY, CALIFORNIA 94720*